

1 **Revision 1**

2

3

4 **Dry annealing of metamict zircon: a differential scanning calorimetry study**

5

6 ROBERT T. PIDGEON¹, PETER G. CHAPMAN², MARTIN DANIŠÍK¹ and
7 ALEXANDER A. NEMCHIN¹

8

9 1 Department of Applied Geology, Curtin University, Bentley, Western Australia

10 2 Department of Chemistry, Curtin University, Bentley, Western Australia

11

12

13 **Abstract**

14

15 We report the results of a Differential Scanning Calorimeter (DSC) study of the annealing
16 of a metamict Sri Lankan zircon. Raman measurements on most chips of the powdered
17 zircon starting material, Sri Lankan zircon (WZ19), showed no evidence of a crystalline
18 structure whereas a few chips retained residual Raman bands typical of highly radiation
19 damaged zircon. DSC runs on aliquots of the powdered sample were heated to 850°C and
20 1000°C at rates of 2°C and 10°C/minute and to 1500°C at a rate of 10°C/minute. Raman
21 spectroscopy was used to investigate the crystallinity of grains at selected temperature
22 stages. Exothermal peaks were observed at about 910°C and 1260°C during the DSC run
23 to 1500°C. The 910°C peak was demonstrated by Raman spectroscopy to mark the
24 crystallization of tetragonal zirconia and the exothermic peak at about 1260°C was
25 demonstrated to represent the reaction of zirconia and amorphous silica to form
26 crystalline zircon. The degree of crystallinity of these grains was almost identical to that
27 of highly crystalline zircons from recent gem gravels from New South Wales. A small
28 number of experimental chips from DSC analyses under 1000°C were found to have
29 zircon Raman bands that indicated they had undergone partial annealing.

30

31

32

33 Key words: radiation damage, metamict zircon, radiation damage annealing, Differential
34 Scanning Calorimeter, zircon Raman spectra

35

36

37

38

Introduction

39

40 The breakdown of the zircon structure by the radioactive decay of minor
41 components U and Th and their radioactive daughters has been the subject of research for
42 over fifty years (e.g. Holland and Gottfried 1955; Pabst 1952; Weber 1990; Ewing et al.
43 2003; Zhang et al. 2000; Nasdala et al. 2001; Geisler et al. 2001, and others).
44 Understanding the damage processes and the structural changes of zircon as it evolves to
45 the metamict state is important in explaining discordant results in zircon U-Pb dating,
46 anomalous zircon (U-Th)/He ages (e.g. Guenther et al. 2013), and in estimating the
47 integrity of zircon as a host for the disposal of actinide nuclear waste and predicting the
48 properties of zircon in ceramic applications. The annealing of radiation damaged zircon is
49 equally important in the above fields as well as fission track dating (e.g. Hasebe et al.
50 2003) and has applications in geochronology in its own right (e.g. Pidgeon 2014).

51 Early investigations of zircon radiation damage and annealing used optical (e.g.
52 Vance and Anderson 1972), X-ray diffraction (XRD) techniques (e.g. Holland and
53 Gottfried 1955) and various density and electron microscope (TEM) techniques (e.g.
54 Weber 1990; McLaren et al. 1994; Capitani et al. 2000). Differential thermal analysis has
55 also been applied (Lipova et al. 1965, Kulp et al. 1952) and more recently Raman
56 spectroscopy has proved to be extremely effective in monitoring changes in radiation
57 damage in zircons (Nasdala et al. 1995; Geisler et al. 2001, Zhang et al. 2000). A number
58 of researchers concluded that annealing of metamict zircon takes place in two stages
59 involving first, the formation of zirconia and second, full recrystallization back to the
60 original zircon structure. Weber (1990) reported that annealing of a Pu doped amorphous
61 zircon involved two steps, initial crystallization of pseudo-cubic zirconia at about 1050°C
62 and full density recovery at about 1450°C where the zircons transforms back to its

63 original zircon structure. Colombo and Chrosch (1998) also reported that the recovery of
64 thermally treated metamict Sri Lankan zircon involved two phases, zircon and pseudo-
65 cubic ZrO₂. Váczi et al. (2009) reported that dry annealing of fully metamict zircon
66 involved initial formation of ZrO₂, between 800°C and 1000°C prior to the formation of
67 crystalline zircon above 1150°C. McLaren et al. (1994) also reported the formation of
68 zirconia on dry heating a high U Sri Lankan zircon to 900°C. In the present research our
69 objective was to investigate the progressive annealing and phase changes in metamict
70 zircon during isochronal dry annealing, as determined by a Differential Scanning
71 Calorimeter (DSC) study using Raman spectroscopy to monitor the evolving zircon
72 crystal structure.

73

74

The zircon sample

75

76 The zircon sample used in the study, WZ19, was a black, translucent pebble from
77 the Sri Lankan alluvial deposits. The U and Th concentrations of the pebble, determined
78 on an aliquot of the powdered sample, are 9902 ppm and 2296 ppm respectively by
79 isotope dilution ICP-MS. The α -dose experienced by the zircon was $13.2 \times 10^{15} \alpha/\text{mg}$,
80 determined from the U and Th concentrations and a “radiation damage age” for Sri
81 Lankan zircons of 375 Ma (Palenik et al. 2003). The radiation damage age is defined as
82 the time needed to generate the observed radiation damage and takes into account the
83 realisation that the Sri Lankan zircons have been annealed since their formation (e.g.
84 Nasdala et al. 2001, 2004; Garver 2002). The method for determination of radiation
85 damage ages has been described by Pidgeon (2014). Previous reports where α -doses have
86 been determined using the 560 Ma U-Pb age of Sri Lankan zircons (e.g. Zhang et al.
87 2000) give α -doses that are in excess of that needed to generate the observed damage.
88 The α -doses in these reports need to be adjusted down by about 0.55 (Nasdala et al.
89 2004). For example the α -dose of $23.5 \times 10^{15} \alpha/\text{mg}$ for the most severely radiation
90 damaged Sri Lankan zircon, sample 82988, reported in Table 1 of Zhang et al. (2000),
91 would be reduced to $12.9 \times 10^{15} \alpha/\text{mg}$. Rios et al. (2000) concluded that zircons with a
92 dose higher than about $8 \times 10^{15} \alpha/\text{mg}$ (revised to $4.4 \times 10^{15} \alpha/\text{mg}$) show no further
93 changes in their metamict structure with further bombardment. Murakami et al. (1991)

94 also proposed an α -dose of $8 (4.4) \times 10^{15} \alpha/\text{mg}$ for their Stage III level of radiation
95 damage where zircon appears to be entirely aperiodic as far as can be determined by X-
96 Ray or electron diffraction. An α -dose of 12 (revised to $6.6) \times 10^{15} \alpha/\text{mg}$ was found by
97 Holland and Gottfried (1955) to correspond with the disappearance of zircon XRD peaks.
98 Weber (1990) noted that TEM studies of natural zircon confirm that an α -dose of 6.5 to
99 9.5 (revised to 3.6 to 5.2) $\times 10^{15} \alpha/\text{mg}$ will result in complete amorphization of zircon.
100 Zircon WZ19 used in the present study, with an effective α -dose of $13.2 \times 10^{15} \alpha/\text{mg}$
101 (from the time of zircon annealing), is far in excess of these values and of the same order
102 as sample 82988 of Zhang et al. (2000), indicating it has a fully aperiodic structure.
103 However, as rare chips of the powdered sample have residual “Raman” bands it is evident
104 that the zircon is not homogeneous but has some lower U zones that are highly damaged
105 but not entirely metamict.

106

107

Analytical methods

108

109 In the present study samples were analysed with a TA Instruments SDT Q600
110 simultaneous DSC-TGA in a nitrogen atmosphere flowing at 100 ml/minute. The heat
111 flow between the sample and reference crucibles was calibrated using a sapphire disc
112 provided by the instrument manufacturer. This allows the differential temperatures to be
113 converted into heat flow. The sample aliquot and reference (an empty alumina pan) are
114 heated at the same rate and the temperature difference between them is recorded.
115 Powdered ~50 mg aliquots of zircon pebble WZ19 were placed in a 90 μL alumina
116 crucible and annealing experiments were run over (1) a temperature range of 25°C to
117 850°C and (2) a temperature range of 25°C to 1000°C with heating rates of 10°C/minute
118 and 2°C/minute (these runs were made on a different instrument: see accompanying
119 material) and a temperature range of 25°C to 1500°C, with a heating rate of 10°C/minute
120 (Fig.1). Raman spectra were determined on ten individual grains of the powdered Sri
121 Lankan zircon (WZ19) starting material and sample chips from the DSC runs. Typical
122 Raman Spectra are shown on Figs 2, and 3.

123

124

Raman spectra were collected at room temperature with an ISA LabRam
dispersive Raman spectrometer at the Department of Chemistry at Curtin University

125 using the 632.817 nm line of a HeNe laser and a beam power of 2 mW at the sample. The
126 scattered Raman light was analysed with a charge coupled device (CCD) detector after
127 being dispersed by a grating of 1800 grooves per mm. A 50x objective was used on a
128 BX-40 microscope. The spectral resolution of $\sim 1.9 \text{ cm}^{-1}$ was determined from FWHM
129 measurements of the Neon Raman bands. The Raman shift positions were calibrated
130 against the 520.7 cm^{-1} Silicon Raman band. Counting times were between 15 and
131 200 seconds depending on the structural state of the sample.

132 One Raman analysis was made on each of twenty selected zircon fragments
133 (chips) from the reacted powdered sample after each DSC run.

134

135 **Results**

136

137 **The unheated zircon.**

138

139 Raman analyses were made on twenty chips of the powdered zircon sample
140 WZ19. Five representative Raman spectra are shown on Fig. 2A. Most analyses (e.g. 4, 5,
141 and 2) form irregular traces with no zircon Raman bands and are consistent with an
142 amorphous structure. The spectra show broad mounds at 450 to 650 cm^{-1} and 850 to
143 1050 cm^{-1} suggesting some structural memory survives. Zhang et al. (2000) suggest such
144 mounds indicate coexistence of an amorphous structure with embedded damaged
145 crystalline material. The analysis on chip 3 shows residual zircon Raman peaks which
146 indicate that this chip is highly radiation-damaged but not to the extent of the other chips.
147 The analysis on chip 1 also shows small residual zircon Raman peaks which indicates a
148 residual crystallinity. This demonstrates that zircon sample WZ19 is not homogeneous,
149 but has minor domains with residual crystal structure within the main metamict body of
150 the crystal. The measured U and Th contents of aliquots of the powdered sample therefore
151 represent average values.

152

153 **DSC analyses**

154

155 The trace of heat flow versus temperature for the DSC analysis on a 60 mg aliquot
156 of the WZ19 zircon powder heated to 1500°C at 10°C/minute is shown on Fig. 1. The
157 trace shows two exothermic peaks at 910°C and 1260°C. The first sharp peak shows a
158 rapid rise from 897°C to 910°C and a tail to ~920°C. The recorded heat release is 41 J/g.
159 The second broader and flatter peak shows a rise from about 1185°C to 1260°C and a tail
160 to about 1350°C. The recorded heat release of this peak is 49 J/g. Further DSC runs to
161 850°C and 1000°C were made at a heating rate of 2°C/minute (see accompanying
162 material)

163 Representative Raman spectra of chips (20 measured) from runs to 850°C and
164 1000°C are shown on Fig. 2. Four of the five spectra on Fig. 3A, (to 850°C) show no
165 zircon or other Raman bands but resemble the irregular spectra of unheated metamict
166 zircon on Fig. 1, except that the broad mounds from 450-650 cm⁻¹ and 850-1050 cm⁻¹ are
167 more defined than comparative structures on the Raman spectra in Fig. 1. This clearly
168 demonstrates that the metamict structure has undergone additional ordering as the
169 temperature has risen to 850°C. There is no evidence of any thermal peaks that might
170 suggest a phase change or reaction in the sample below 850°C.

171 One Raman analysis (WZ19b-2)(Fig. 2B) from the 850°C run shows definite
172 zircon (and some anomalous) bands. In this spectrum the zircon ν₃(SiO₄) stretching
173 vibration has a peak position of 1003.7 cm⁻¹ and a FWHM of 12.5 cm⁻¹ (Fig. 5). We
174 interpret this as a partial recovery of a highly damaged, but not completely metamict,
175 domain in the WZ19 zircon, such as shown by the spectrum for unheated chip WZ19A-3
176 in Fig. 2A.

177 Six Raman spectra of chips heated to 1000°C are presented on Fig. 2C. Also
178 shown on this figure is a representative Raman spectrum of a highly crystalline “Mud
179 Tank” zircon. It is most striking that all Raman spectra contain numerous peaks that are
180 not characteristic of zircon. These peaks are interpreted as indicating a new mineral phase
181 that formed between the temperatures 850°C and 1000°C, clearly coinciding with the
182 exothermal peak at about 910°C. A representative Raman spectrum, WZ19C-3 from Fig.
183 2B, and the Raman spectrum of tetragonal zirconia (from Mercer et al. 2007) are shown
184 on Fig. 3. The two spectra are similar, and include lines at 148 cm⁻¹ and 263 cm⁻¹ that are
185 not present in the monoclinic zirconia spectrum and do not have a line at 348cm⁻¹ that is

186 peculiar to the monoclinic phase. The cubic zirconia spectrum has far fewer lines than the
187 zirconia spectra shown on Fig. 3 (Phillippi and Mazdidasni 1971). We conclude from the
188 Raman spectra that the exothermic peak observed at about 910°C represents the rapid
189 crystallization of tetragonal zirconia. Definite zircon peaks are present in the spectra of
190 WZ19C-1 and C-6. These data are shown on Fig. 5 to fall well away from those of the
191 recrystallised grains (see following) and off the trend through the Permian rhyolite – River
192 gem-gravel zircons. This is interpreted as indicating a recovery rather than a
193 recrystallisation of highly radiation damaged zircon.

194 Also striking are the Raman spectra (Fig. 4) of sample chips after heating to
195 1500°C. Six of the seven representative Raman spectra shown on Fig. 4 have strongly
196 crystalline zircon Raman spectra together with remnants of the previously dominant
197 zirconia peaks. This demonstrates that zirconia and amorphous silica have recrystallised
198 to form zircon between 1000°C and 1500°C and it is evident that this reaction coincides
199 with the exothermic phase change observed in the DSC analysis at about 1260°C (Fig. 1).
200 The Raman shift positions and FWHM of ten of the spectra are shown on Fig. 5. Also
201 shown on this figure are Raman data from unannealed, Permian rhyolite zircons from
202 Nasdala et al. (1998) and highly crystalline zircon pebbles from river gem gravels from
203 the slopes of Tertiary volcanoes in New South Wales. These are the most crystalline
204 zircons known to the present authors. The recrystallised WZ19 zircon grains form a tight
205 group on Fig. 5 demonstrating that metamict WZ19 zircon grains have undergone
206 uniform recrystallization during the DSC run and the degree of crystallinity of the grains
207 is only slightly less than the highly crystalline river gravel zircons.

208 The spectra on Fig. 4 are arranged to show the increasing presence of unassigned
209 peaks. The peak at about 300 cm⁻¹ on spectra WZ19-10 could be remnant zirconia peak.
210 However, the large peak at about 680 cm⁻¹ and other minor anomalous peaks in the
211 WZ19-6 spectrum have not been identified. This peak is not cubic zirconia which would
212 show as a broad peak at about 625 cm⁻¹ (Phillippi and Mazdidasni 1971). We tentatively
213 interpret these as anomalous luminescence bands.

214

215

Discussion

216

217 Our DSC and Raman analyses demonstrate that the annealing path of metamict
218 zircon is marked by two phase changes, first the crystallization of metastable tetragonal
219 zirconia at a temperature of about 897°C to 920°C and second the recrystallization of
220 nearly undamaged zircon at 1185°C to 1260°C. It is interesting to note that in an early
221 Differential Thermal Analysis (DTA) study of metamict zircons Kulp et al. (1952)
222 identified an exothermic “doublet” reaction at about 900°C but were unable to explain the
223 cause. Our results confirm previous reports of a two-stage process in the crystallization of
224 metamict zircon involving initial stages of zirconia formation followed by a second stage
225 of formation of crystalline zircon (e.g. Weber 1990; Weber et al. 1994; Capitani et al.
226 2000). Capitani et al. (2000) reported that, on dry heating highly amorphosed zircons,
227 ZrO₂ grains were detected at 930°C and small zircon grains were observed after 16 hours
228 at 1330°C. Capitani et al. (2000) and McLaren (1994) also reported zirconia formation in
229 less radiation damaged zircon after dry heating to about 900°C although in detail zirconia
230 formation may relate to amorphous domains in these grains.

231 Of these reports the two isochronal annealing studies most closely related to our
232 DSC study are those of (1) Vance and Anderson (1972), who reported crystallization of
233 tetragonal zirconia during isochronal annealing experiments on metamict zircon where
234 the grain size was recorded as 100 Å after heating for one hour at 850-950°C and 500 Å
235 after heating for 1 hour at 1100°C; and (2) Weber (1990, 1991) who reported XRD and
236 density data for an isochronal annealing study of an amorphous Pu-doped zircon with
237 anneals carried out for 12 hrs at 100°C intervals from 200-900°C, 50°C intervals from
238 900°C to 1250°C and 100°C intervals to 1600°C. The first recovery stage was a density
239 increase coincident with XRD evidence for the presence of pseudo-cubic zirconia. The
240 second stage of recovery is associated with transformation back to the original zircon
241 structure as measured by the density before or at the 1450°C temperature step. McLaren
242 et al. (1994) and Capitani et al. (2000) also observed growth of zirconia grains from
243 metamict zircon at about 900°C and Vance (1975) reported full recovery of the infrared
244 spectrum of a metamict zircon at 1450°C.

245 In our results the broad exothermic peak from about 1185°C to 1350°C (Fig. 1)
246 marks the reaction between zirconia and amorphous silica to form crystalline zircon
247 (Figs. 2 and 5). It can be seen from Fig. 5 that the crystallised zircon is not quite

248 complete, as compared to the data points of the gem gravel zircons, but extends along the
249 trend of slightly radiation damaged zircon indicated by the distribution of data points
250 from unannealed zircon from a Permian rhyolite (Nasdala et al. 1998). We attribute this
251 to the incorporation of defects into the rapidly crystallising zircon lattice during the DSC
252 run with a temperature increase of 10°C/ minute. The extended temperature range of the
253 exothermic peak from about 1185°C to 1350°C (Fig. 1) contrasts with the sharp
254 exothermic peak of the first annealing stage (Fig.1). This could be due to kinetic factors
255 such as diffusion rates of ions moving from defect to lattice positions or as a consequence
256 of the heterogeneity of disorder in the amorphous zircon, where energy required for
257 zircon crystallization is lower in relatively less disordered domains than that in more
258 highly disordered domains.

259 The enthalpy of reaction of the formation of zircon from its constituent oxides has
260 been determined by Ellison and Navrotsky (1992) as -27.9 kJ/mol. However, given the
261 starting material of quartz and spectroscopic grade ZrO₂ used in this determination the
262 results may have little relevance to the reconstitution of zircon from the amorphous silica-
263 zirconium mixture present in metamict zircon. More relevant is the enthalpy
264 determinations of zircon formation from radiation damaged zircon by Ellsworth et al.
265 (1994) who reported enthalpy determinations of zircon annealing using drop calorimetry
266 at a temperature of 1000°C, for a number of radiation damaged zircons including
267 metamict Sri Lankan zircon 6500 which contains about 7600 ppm of equivalent U and
268 has an α -dose of 11.7 (corrected to 6.4) x 10¹⁵ α /mg. After heating to 1000°C an aliquot
269 of zircon 6500 showed only zirconia XRD peaks, which is in accord with the present and
270 previous studies that show a higher temperature is required for zircon recrystallization.
271 The measured enthalpy of this reaction was -55 kJ/mol. Ellsworth et al. (1994) comment
272 that if sample 6500 had annealed to only ZrO₂ (tetragonal) and SiO₂ (glass) “the
273 measured enthalpy should be -16.6 kJ/mol, suggesting that most of sample 6500 must
274 have annealed to a state energetically similar to crystalline zircon”. Whereas this is
275 difficult to reconcile with our DSC results, which show stage 2 recrystallization to zircon
276 above 1100°C, the heat emission for our stage 1 crystallization of zirconia of 40 J/g (Fig.
277 1), equated to an enthalpy of -5 kJ/mol, is far lower than the enthalpy values reported by
278 Ellsworth et al. (1994). The interpretation of our thermal data as an enthalpy value

279 assumes that all zirconium has taken part in the reaction which is probably not correct as
280 we know zircon WZ19 has domains with residual crystallinity. Even with as much as
281 20% of the zirconium unavailable our estimate of the enthalpy of the reaction of up to -6
282 kJ/mol is significantly lower than the Ellsworth et al. (1994) estimate. This discrepancy is
283 at present unexplained. Our estimate for the enthalpy of stage 2, the crystallization of
284 zircon, is similar to stage 1 but will require further confirmation as areal integration of
285 this broad, flat exothermal peak (Fig. 1) is susceptible to uncertainty in the choice of the
286 baseline.

287 No exothermal peaks were observed in the DSC run up to 850°C suggesting that
288 the recovery process up to this point does not involve phase changes or specific reaction.
289 This is also shown in Raman measurements on most chips heated to 850°C which retain
290 amorphous Raman spectra however, strong zircon Raman peaks have been identified in
291 one chip, WZ19B-2 in the run to 850°C (Fig. 2B) and Raman peaks have been identified
292 in the zirconia dominated spectra of chips WZ19C-1, 5 and 6 in the run to 1000°C (Fig.
293 5). Raman data of these grains are included in a table in the accompanying material. On
294 Fig. 5 it can be seen that data points fall well away from the cluster of annealed zircon
295 points and away from the trend through the points and the unannealed Permian rhyolite
296 zircon data points of Nasdala et al. (1998). This demonstrates a process of annealing very
297 different from that observed in the other grains and is interpreted to represent partial
298 recovery of less damaged, possibly lower U, domains in the parent zircon crystal, such as
299 illustrated by the Raman spectrum of unheated chip WZ19A-3 on Fig. 2A. These results
300 demonstrate that recovery of partially metamict zircon, that has a remnant crystalline
301 structure, is active by 850°C.

302 These observations are in accord with the results of experiments at lower
303 temperatures (e.g. Geisler et al. 2001), where annealing of highly radiation damaged
304 zircon occurs by progressive removal of defects. Geisler et al. (2001) reported the results
305 of a series of dry heating experiments on two partially metamict Sri Lankan zircons that
306 consist of misoriented disordered crystalline domains within an amorphous matrix as
307 revealed by TEM studies (e.g. Bursill and Mc Laren, 1966; Murakami et al. 1991; Weber
308 et al. 1994; Capitani et al. 2000). At temperatures from 600°C to 900°C and durations
309 from 1 minute to 200 hours, recovery of the zircon structure measured, by the Raman

310 peak position and line width (FWHM) of the $\nu_3(\text{SiO}_4)$ stretching vibration did not follow
311 the initial correlation trend observed during the accumulation of radiation damage, where
312 line-width increased systematically with decreasing phonon frequency (Geisler et al.
313 2001) (see Fig. 5). Instead, heating experiments showed that the $\nu_3(\text{SiO}_4)$ Raman peak
314 increased in intensity and showed a rapid initial recovery of the phonon frequency
315 compared to a slower recovery of the line width. Geisler et al. (2001) interpreted this as
316 evidence that the first stage in the recovery of the radiation-damaged zircon structure is
317 the recovery of the short-range order by the removal of point defects in the crystalline
318 domains and at this stage recrystallization of amorphous zircon is limited or not activated
319 at all (Geisler et al. 2001). The anomalous positions of Raman shift and FWHM data of
320 grains from DSC runs up to 1000°C on Fig. 5 can be readily explained by a rapid
321 recovery of the Raman shift but slower recovery of the Raman peak as demonstrated
322 experimentally by Geisler et al. (2001). These results support our and previous
323 conclusions that annealing of amorphous zircon and the recovery of partially radiation
324 damaged zircon are two separate processes. These observations also confirm reports that
325 propose two stages in the annealing process involving firstly the recovery of heavily
326 disturbed but still crystalline domains and secondly the recrystallization of amorphous
327 regions (Colombo and Chrosch, 1998).

328
329

330 **Implications**

331

332 Results of our DSC study of the annealing of a metamict zircon provide enthalpy
333 and reaction-temperature information for phase changes at 900-915°C and 1185-1350°C,
334 that have been identified from Raman measurements to represent initial crystallization of
335 tetragonal zirconia followed by recrystallization of zirconia and amorphous silica to form
336 undamaged zircon. This confirms previous reports of two-stage annealing of metamict
337 zircon involving the formation of zirconia followed at higher temperature by
338 recrystallization to undamaged zircon. This annealing process can be distinguished from
339 the recovery of partially metamict zircon described by Geisler et al. (2001) and could
340 form the basis for a definition of “amorphous” zircon as “zircon that has such a high

341 degree of radiation damage that recrystallization involves initial formation of metastable
342 zirconia followed at a higher temperature by crystallization of zirconia and amorphous
343 silica to form undamaged zircon“. This is not to imply that structural differences within
344 an amorphous region do not exist (Rios et al. 2000). Our results and previous studies are
345 important for nuclear waste applications where zircon has been proposed as a host
346 mineral for long-term storage of actinides. If, in such a facility zircon broke down to an
347 amorphous state, as shown by Weber (1991) can happen in a few years to a Pu-doped
348 zircon, its resistance to water penetration and possible actinide loss is greatly reduced
349 (Geisler et al. 2003). Our results show that it would be impractical to recrystallise the
350 amorphous zircon back to its undamaged crystalline form. Amorphous zircon is highly
351 susceptible to loss of Pb and He severely limiting its usefulness in geochronology.
352 Recrystallization of amorphous zircon on the other hand would most likely reset the
353 geochronological systems as well as the crystal structure establishing a time zero point
354 for geochronological measurements, including zircon fission track, radiation damage and
355 (U-Th)/He dating. However, as far as the authors are aware there have been no reports of
356 evidence such as multiple zirconia inclusions in zircon from natural settings that could
357 indicate that annealing of “amorphous” zircon has taken place. This suggests that
358 annealing of amorphous zircon is rare in dry geological environments which is in accord
359 with our result as even in granulite to eclogite facies metamorphism temperatures rarely
360 rise to 900°C.

361 However, a factor that can seriously affect the annealing behaviour of radiation
362 damaged zircon is the presence of water (Geisler et al. 2004). Geisler et al. (2004)
363 reported the formation of monoclinic zirconia in hydrothermally treated metamict Sri
364 Lankan zircon at a temperature of 400°C demonstrating the profound influence of water
365 in lowering the activation energy for zirconia formation. The formation of zirconia in
366 these hydrothermal experiments also demonstrates that the annealing of amorphous
367 zircon takes place as a two stage process whether under dry or hydrothermal conditions.
368 These results indicate that annealing of amorphous zircon to zirconia and then crystalline
369 zircon is possible under natural metamorphic conditions where water is present.

370 Our DSC experiment provides a means for investigating the annealing and
371 recovery of radiation damaged materials. The DSC runs can be stopped at any

372 temperature providing a continuous record of the stages of annealing of a metamict zircon
373 or other radiation damaged mineral. This provides an opportunity to study reactions and
374 configurations of zirconium, silicon, oxygen and trace elements at the atomic scale at
375 selected stages in the annealing process. It also provides an opportunity to measure the
376 electrical and other properties of the amorphous zircon as it progressively anneals.

377

378 **Acknowledgments**

379

380 We wish to thank T. Geisler and an anonymous reviewer for their constructive
381 reviews. We thank R. Pogson of the Australian Museum in Sydney for the opportunity to
382 make Raman measurements on NSW gem gravel zircons. RTP acknowledges support
383 from the Division of Engineering and Science.

384

385 **References**

386

387 Bursill, L.A. and McLaren, A.C. (1966) Transmission Electron Microscope Study of
388 Natural Radiation Damage in Zircon ($ZrSiO_4$). *Physica Status Solidi*, 13, 331-343.

389

390 Capitani, G.C., Leroux, H., Doukhan, J.C., Rios, S., Zhang, M., and Salje, E.K.H. (2000)
391 A TEM investigation of natural metamict zircons: structure and recovery of amorphous
392 domains. *Physics and Chemistry of Minerals*, 27, 545-556.

393

394 Colombo, M., and Chrosch, J. (1998) Annealing of natural metamict zircons: II high
395 degree of radiation damage. *Radiation Physics and Chemistry*, 53, 563-566.

396

397 Ellison, A.J.G. and Navrotsky, A. (1992) Enthalpy of formation of zircon. *Journal of the*
398 *American Ceramic Society*, 75, 1430 – 1433.

399

400 Ellsworth, S., Navrotsky, A. and Ewing, R.C. (1994) Energetics of Radiation Damage in
401 Natural Zircon (ZrSiO₄). *Physics and Chemistry of Minerals*, 21, 140-149.

402

403 Ewing, R.C., Meldrum, A., Wang, L.M., Weber, W.J., and Corrales, L.R. (2003)
404 Radiation effects in zircon. In: *Zircon, Reviews in Mineralogy and Geochemistry*, vol.53,
405 J.M.Hancher and P.W.O. Hoskin (Editors), 387-425.

406

407 Garver, J.I. (2002) Discussion: "Metamictisation of natural zircon: accumulation versus
408 thermal annealing of radioactivity-induced damage" by Nasdala et al. 2001
409 (*Contributions to Mineralogy and Petrology* 141:125-144). *Contributions to Mineralogy*
410 *and Petrology*, 143, 756-757.

411

412 Geisler, T., Pidgeon, R.T., van Bronswijk, W., and Pleysier, R. (2001) Kinetics of
413 thermal recovery and re of partially metamict zircon: a Raman spectroscopic study.
414 *European Journal of Mineralogy*, 13, 1163-1176.

415

416

417 Geisler, T., Seydoux-Guillaume, A., Wiedenbeck, M., Wirth, R., Berndt, J., Zhang, M.,
418 Mihailova, B., Putnis, A., Salje E.K.H. and Schlüter, J. (2004) Periodic precipitation
419 pattern formation in hydrothermally treated metamict zircon. *American Mineralogist*, 89,
420 1341-1347.

421

- 422 Guenther, W.R., Reiners, P.W., Ketcham, R.A., Nasdala, L., and Gierster, G. (2013)
423 Helium diffusion in natural zircon: Radiation damage, anisotropy, and the interpretation
424 of zircon (U-Th)/He thermochronology. *American Journal of Science*, 313(3), 145-98.
425
- 426 Hasebe, N., Mori, S., Tagami, T., and Matsui, R. (2003) Geological partial annealing
427 zone of zircon fission-track system: additional constraints from the deep drilling MITI-
428 Nishikubiki and MITI-Mishima. *Chemical Geology*, 199, 45-52.
429
- 430 Holland, H., and Gottfried, D. (1955) The effect of nuclear radiation on the structure of
431 zircon. *Acta Crystallographica*, 8, 291-300.
432
- 433 Kulp, J.L., Volchok, H.L. and Holland, H.D. (1952) Age from metamict minerals. *The*
434 *American Mineralogist*, 37, 709-718.
435
- 436 Lipova, I.M., Kusnetsova, G.A., and Markarov, Ye S. (1965) An investigation of the
437 metamict state in zircons and cyrtolites. *Geochemistry International* 2, 513-525
438 (Geokhimiya 6, 681-694)
439
- 440 McLaren, A.C., Fitz Gerald, J.D., and Williams, I.S. (1994) The microstructure of zircon
441 and its influence on the age determination from Pb/U isotope ratios measured by ion
442 microprobe. *Geochimica et Cosmochimica Acta*, 58, 993-1005.
443

- 444 Mercer, C., Williams, J.R., Clarke, D.R., and Evans, A.G. (2007) On a ferroelastic
445 mechanism governing the toughness of metastable tetragonal-prime yttria-stabilised
446 zirconia. *Proceedings of the Royal Society A*, 463, 1393-1408.
- 447
- 448 Murakami, T., Chakoumakos, B.C., Ewing, R.C., Lumpkin, G.R., and Weber, R.W.
449 (1991) Alpha-decay event damage in zircon. *American Mineralogist*, 76, 1510-1532.
- 450
- 451 Nasdala, L., Irmer, G., and Wolf, D. (1995) The degree of metamictization in zircon: a
452 Raman spectroscopic study. *European Journal of Mineralogy*, 7, 471-478.
- 453
- 454 Nasdala, L., Götze, J., Pidgeon, R.T., Kempe, U., Seifert, T. (1998) Constraining a
455 SHRIMP U–Pb age: micro-scale characterization of zircons from Saxonian Totliegen
456 rhyolites. *Contrib. Mineral. Petrol.* 132, 300–306.
- 457
- 458 Nasdala, L., Reiners, P.W., Garver, J.I., Kennedy, A.K., Stern, R., Balan, E., and Wirth,
459 R. (2004) Incomplete retention of radiation damage in zircon from Sri Lanka, *American*
460 *Mineralogist*, 89, 219-231.
- 461
- 462 Nasdala, L, Wenzel, M., Vavra, G., Irmer, G., Wenzel, T., and Kober, B. (2001)
463 Metamictisation of natural zircon: accumulation versus thermal annealing of radioactivity
464 – induced damage. *Contributions to Mineralogy and Petrology*, 141, 125-144.
- 465
- 466 Pabst, A. (1952) The metamict state. *American Mineralogist*, 37, 137-157.

467

468 Palenik, C.S., Nasdala, L., and Ewing, R.C. (2003) Radiation damage in zircon.
469 American Mineralogist, 88, 770-731.

470

471 Phillippi, C.M., and Mazdiyasi, K.S. (1971) Infrared and Raman spectra of zirconia
472 polymorphs. Journal of the American Ceramic Society. 54, 254-258.

473

474 Pidgeon, R.T. (2014) Zircon radiation damage ages. Journal of Chemical Geology, 367,
475 13-22.

476

477 Rios, S., Salje, E.K.H., Zhang, M. and Ewing, R.C. (2000) Amorphization in zircon:
478 evidence for direct impact damage. Journal of Physics: Condensed Matter. 12, 2401-
479 2412.

480

481 Váczi, T., Nasdala, L., Wirth, R., Mehofer, M., Libowitzky, E., and Häger, T. (2009) On
482 the breakdown of zircon upon “dry” thermal annealing. Mineralogy and Petrology, 97,
483 129-138.

484

485 Vance, E.R., and Anderson, B.W. (1972) Study of metamict Ceylon zircons.
486 Mineralogical Magazine, 38, 605-613.

487

488 Weber, W.J. (1990) Radiation-induced defects and amorphization in zircon. Journal of
489 Materials Research, 5, 2687-2697.

490

491 Weber, W.J. (1991) Self-radiation damage and recovery in Pu-doped zircon. Radiation
492 effects and defects in solids, 115, 341-349.

493

494 Weber, W.J., Ewing, R.C., and Wang, L.M. (1994) The radiation-induced crystalline-to-
495 amorphous transition in zircon. Journal of Materials Research, 9, 688-698.

496

497 Zhang, M., Salje, E.K.H., Farnan, I., Graeme-Barber, A., Daniel, P., Ewing, R.C., Clark,
498 A.M., and Leroux, H. (2000) Metamictization of zircon: Raman Spectroscopic study.
499 Journal of Physics- Condensed Matter, 12, 1915-1925.

500

501

502 Figure Captions

503

504 **Figure 1.** DSC profile of 60 mg of powder of zircon WZ19 heated to 1500°C at
505 10°C/minute.

506

507 **Figure 2.** (A) Stacked Raman spectra made on individual chips of the unheated powdered
508 sample of zircon WZ19. (B) Stacked Raman spectra of chips of the sample after heating
509 to 850°C at 2°C/minute. (C) Stacked Raman spectra of chips of the sample after heating
510 to 1000°C at 2°C/minute.

511

512 **Figure 3.** (A) Raman spectrum of chip WZ19C-3 heated to 1000°C at 2°C/minute. (B)
513 Raman Spectrum of tetragonal zirconia from Mercer et al. (2007).

514

515 **Figure 4.** Stacked spectra of Raman analyses on individual chips of the sample after
516 heating to 1500°C at 10°C/min.

517

518 **Figure 5.** Shows Raman shift and width data-points of twenty zircon chips after the
519 DSC run to 1500°C together with points for partially annealed zircon chips after DSC
520 runs to 850°C and 1000°C. Error bars are 1σ . Also shown for reference are Raman data-
521 points of zircons from gem gravels from New South Wales and unannealed zircons from
522 a Permian rhyolite from Saxony, Germany (Nasdala et al. 1998). The approximately
523 linear trend of these data-points, which includes the crystalline zircons from the 1500°C
524 DSC run, defines the “Radiation Damage Trend“ described by Geisler et al. (2001).

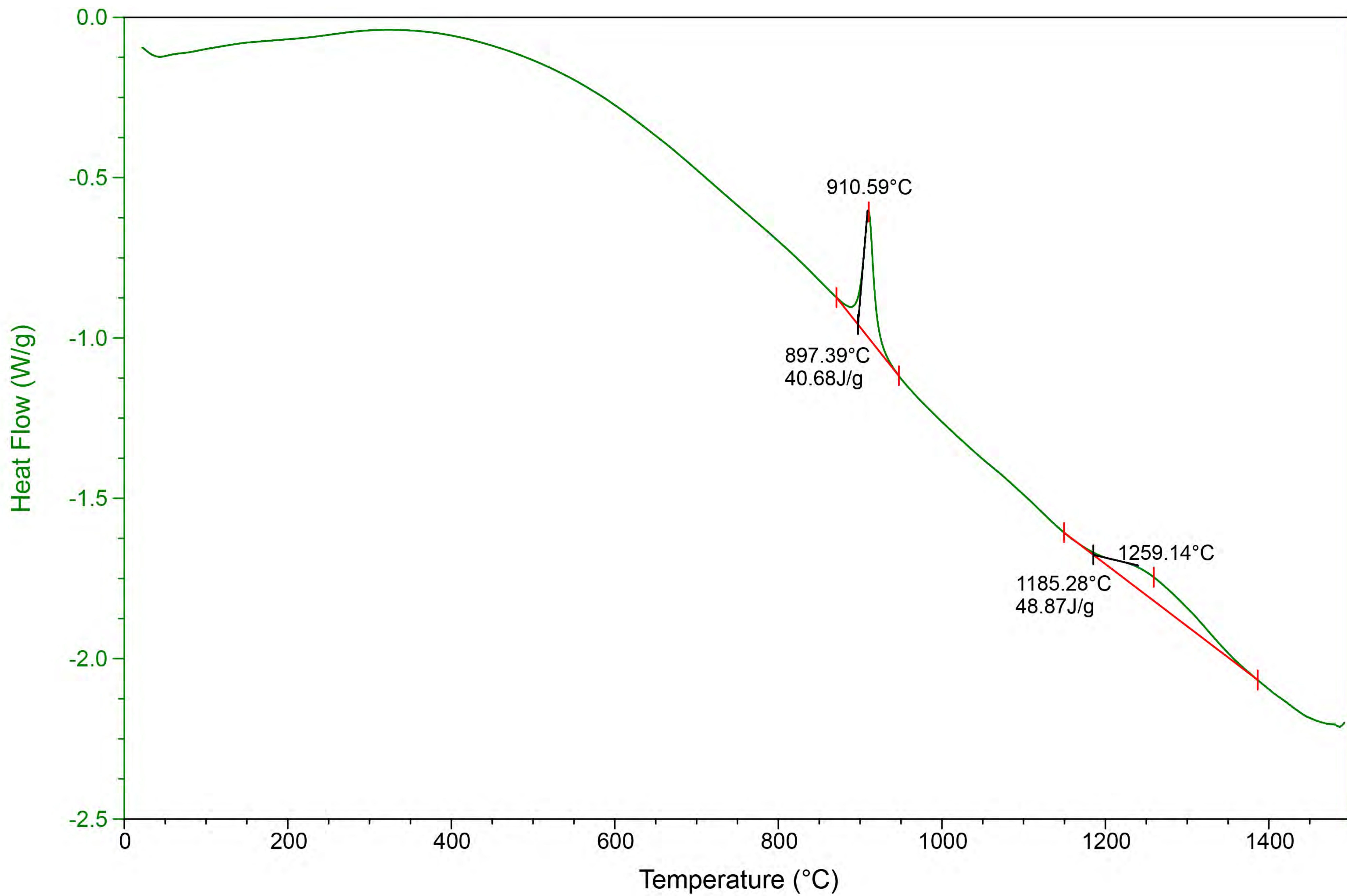


Figure 1

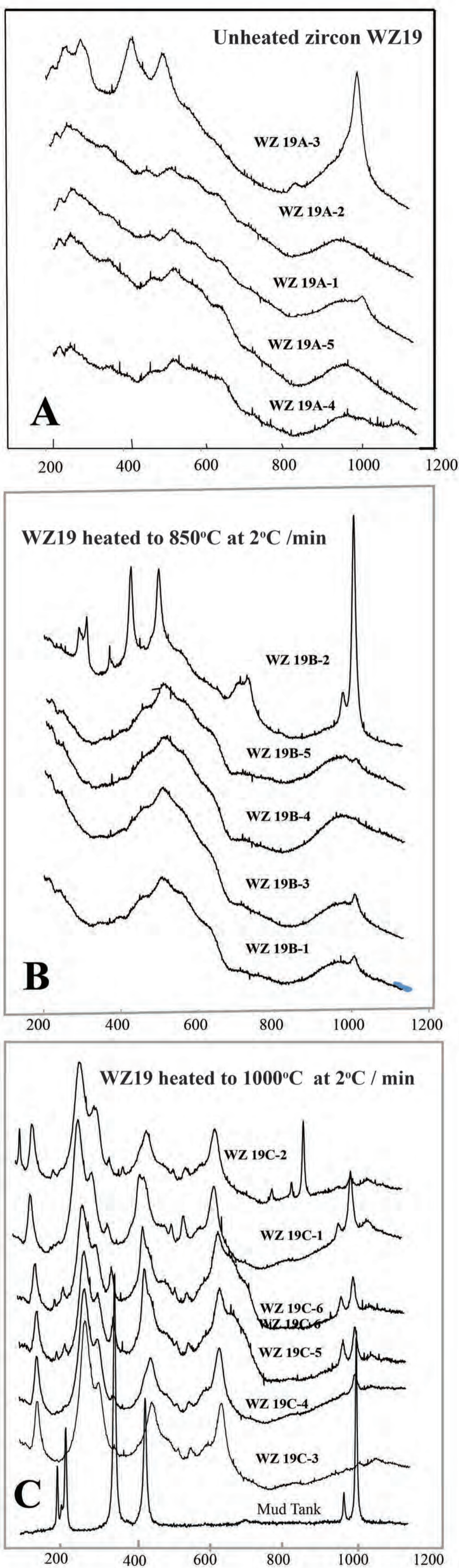


Figure 2

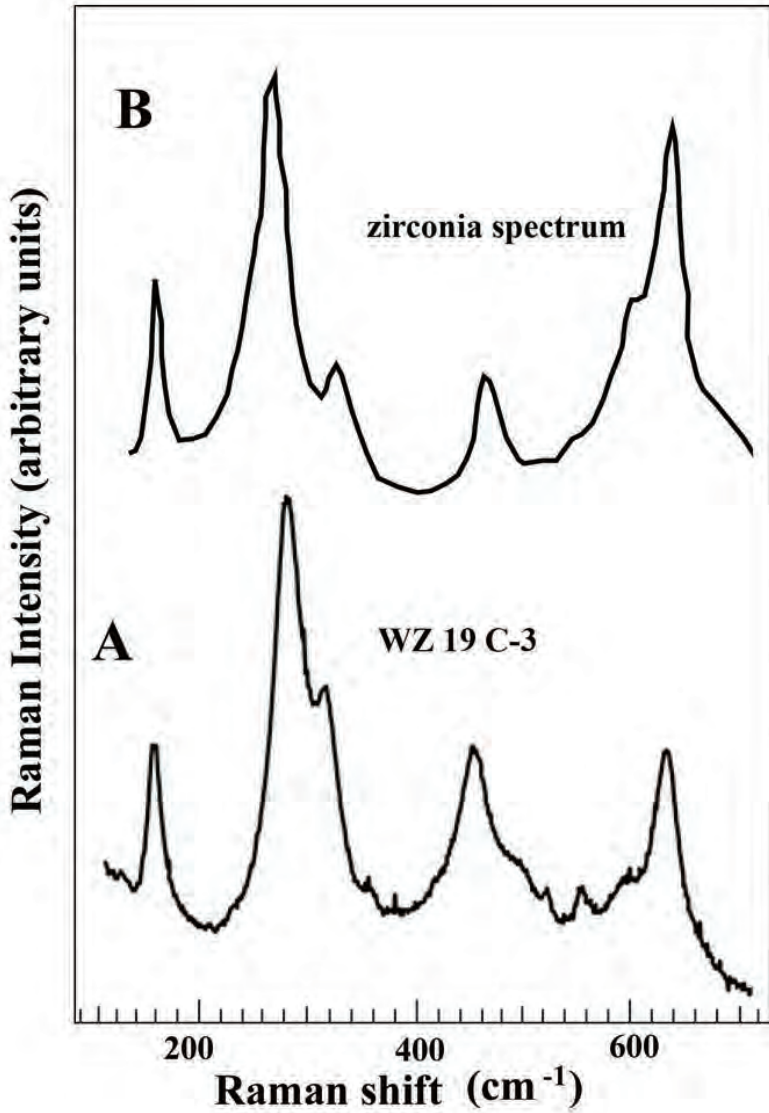


Figure 3

**WZ19 heaed to 1500oC
at 10oC/ min**

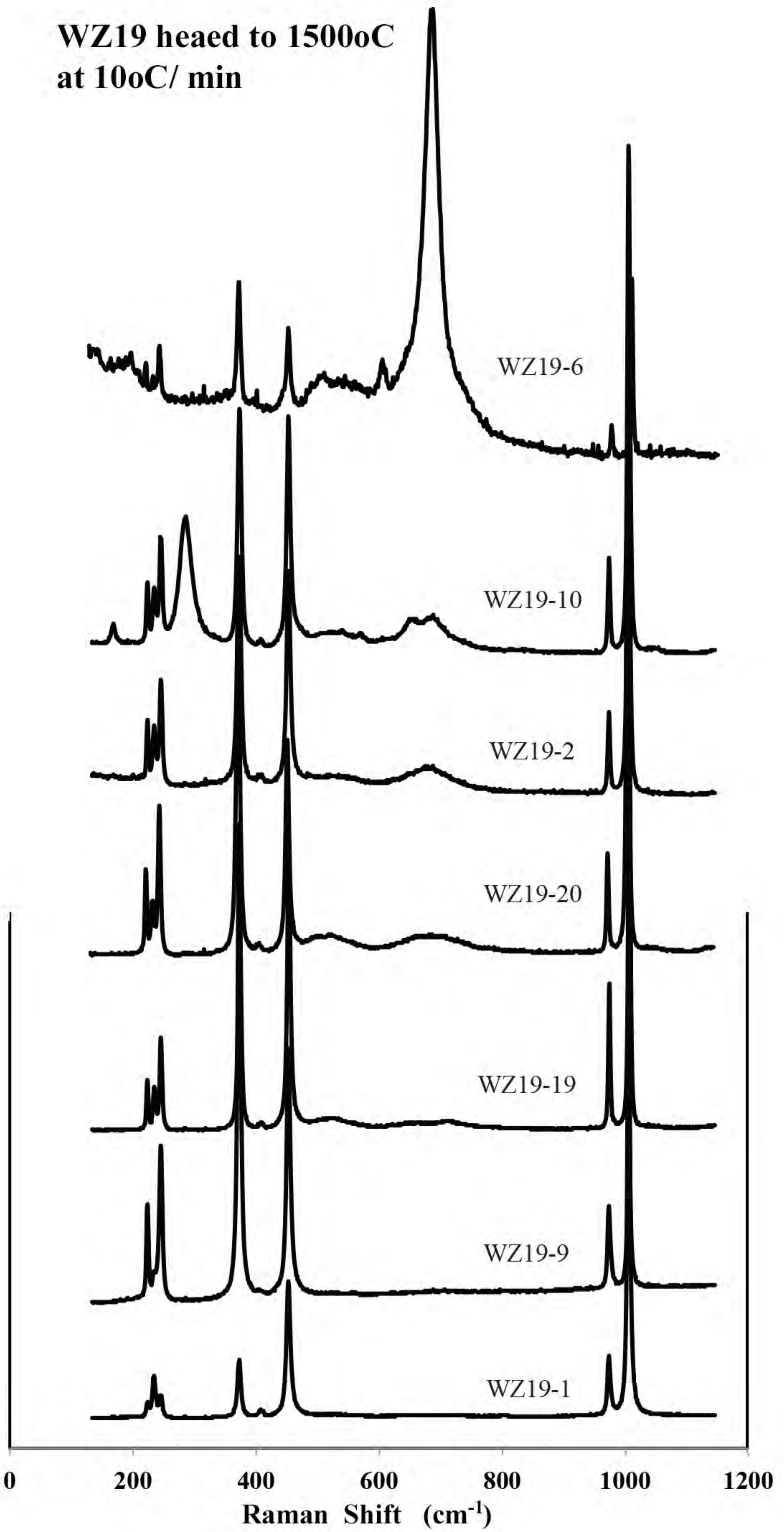


Figure 4

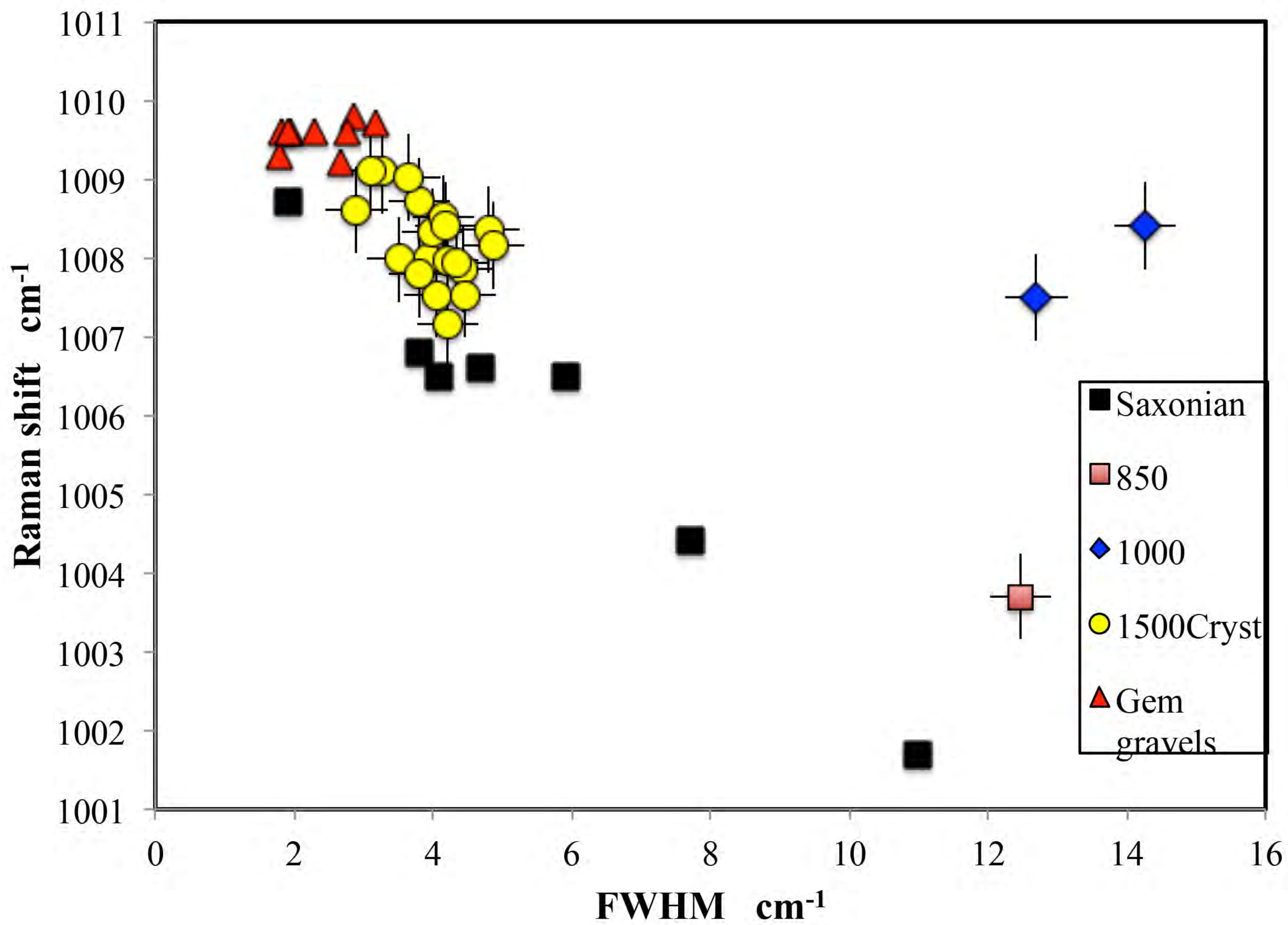


Figure 5